

# Intelligent Optimization Method for CCUS Injection Parameters Based on Improved NSGA-II Algorithm

Honghong Li<sup>1\*</sup>, Yanan Zhang<sup>1</sup>, Bing Chen<sup>1</sup>, Songyan Sang<sup>1</sup>, Hongzhi Han<sup>1</sup>, Miao Liu<sup>1</sup>

1 Kunlun Digital Technology Co, Ltd., Dongcheng, Beijing, 100020

(\*Corresponding Author: lihonghong01@cnpc.com.cn)

## ABSTRACT

In CO<sub>2</sub> enhanced oil recovery (EOR) and sequestration operations, the temperature and pressure of bottomhole fluids play a crucial role in determining CO<sub>2</sub>'s oil solubility and mobility. To achieve optimal EOR and sequestration results, it is essential to design parameters such as injection temperature, pressure, wellbore structure, and insulation materials. To address the issues in designing CCUS injection parameters, this paper proposes a multi-objective intelligent optimization method for CCUS injection parameters based on an improved second-generation Non-dominated Sorting Genetic Algorithm (NSGA-II). First, a CO<sub>2</sub> injection wellbore temperature and pressure calculation model is constructed, enabling the characterization of fluid flow along the wellbore and the simulation of bottomhole temperature and pressure. Subsequently, by introducing an Estimation of Distribution Algorithm (EDA), the randomness and lack of purpose in the crossover and mutation operations of the traditional NSGA-II algorithm are mitigated, thereby enhancing the optimization performance and convergence speed of the algorithm. Finally, through case analysis, the effectiveness and superiority of this intelligent optimization method in designing CCUS injection parameters are validated.

**Keywords:** CCUS, Injection Well, NSGA-II Algorithm, Estimation of Distribution Algorithm

## NONMENCLATURE

### Abbreviations

CCUS	Carbon Dioxide Capture, Utilization, and Storage
EOR	Enhanced Oil Recovery
NSGA-II	Second-generation Non-dominated Sorting Genetic Algorithm

EDA	Estimation of Distribution Algorithm
UMDA	Univariate Marginal Distribution Algorithm
<i>Symbols</i>	
$dQ$	Heat absorption of the infinitesimal segment, W
$dQ_1$	Radial heat flux of the infinitesimal element in the wellbore, W
$dQ_2$	Radial heat flux at the interface between the cement sheath and the formation, W
$dp$	Fluid pressure in the infinitesimal segment of the wellbore, Pa
$dT$	Increased temperature of CO <sub>2</sub> , K
$T_f$	Temperature of CO <sub>2</sub> at a certain depth
$T_h$	Temperature at the interface between the cement sheath and the formation at a certain depth, K
$T_e$	Formation temperature, K
$M$	Mass flow rate of CO <sub>2</sub> , kg/s
$C_p$	Specific heat capacity of CO <sub>2</sub> , J/(kg·K)
$U_{to}$	Overall heat transfer coefficient of the infinitesimal element in the wellbore, W/(m <sup>2</sup> ·K)
$r_{to}$	Outer diameter of the tubing, m
$r_{ti}$	Inner diameter of the tubing, m
$r_w$	Radius of the wellbore, m
$\lambda_e$	Thermal conductivity of the formation, m <sup>2</sup> /s
$\alpha_e$	Thermal diffusivity of the formation, m <sup>2</sup> /s
$g$	Gravitational acceleration, m/s <sup>2</sup>
$\rho$	Density of CO <sub>2</sub> , kg/m <sup>3</sup>
$v$	Flow velocity of CO <sub>2</sub> fluid in the infinitesimal segment, m/s
$\varepsilon$	Average roughness of the tubing, m

$t$	Production time, s
$\theta$	Well deviation angle, °
$f$	Friction factor of the tubing at a certain depth, Dimensionless
$P_{wf}$	Target bottom-hole pressure, MPa
$P'_{wf}$	Calculated bottom-hole pressure, MPa
$T_{wf}$	Target bottom-hole temperature, K
$T'_{wf}$	Calculated bottom-hole temperature, K
$P_{in}$	Injection pressure of CO <sub>2</sub> , MPa
$T_{in}$	Injection temperature of CO <sub>2</sub> , K
$Q_{in}$	Injection rate of CO <sub>2</sub> , t/d

## 1. INTRODUCTION

In the context of the relentless growth of global energy demand and the increasingly severe challenges of climate change, identifying solutions that meet the dual criteria of ensuring energy supply security and reducing greenhouse gas emissions is of paramount importance[1]. The technology of CO<sub>2</sub> Capture, Utilization, and Storage for Enhanced Oil Recovery (CCUS-EOR) has gradually emerged as a vital technological approach to combat climate change, ensure energy security, and promote a green and low-carbon transition[2,3].

The main components involved in CCUS-EOR technology encompass carbon capture, transportation, utilization, and storage. Optimization of injection parameters plays a central role in this technology, being crucial not only for enhancing oil recovery efficiency but also for improving the efficiency of CO<sub>2</sub> storage and ensuring the safety of the storage. Studies have indicated that by optimizing the injection conditions to meet certain requirements, the recovery rate of crude oil can be significantly increased[4]. Moreover, optimizing injection parameters such as bottom-hole pressure and gas injection rate can markedly affect the amount of CO<sub>2</sub> stored[5]. The injection parameters are crucial for the safety of geological CO<sub>2</sub> storage; reasonable injection rates and timing can effectively control the effective stress changes in the reservoir rock, reducing the risk of fracturing in the storage formation[6]. Therefore, by finely tuning the injection parameters, especially the bottom-hole temperature and pressure, one can effectively enhance the CO<sub>2</sub>-enhanced oil recovery and geological storage effects while ensuring the safety of CO<sub>2</sub> storage.

In earlier methods, the pressure and temperature of the injection well were calculated separately, which had

a certain impact on the accuracy of the bottom-hole flow temperature and pressure state calculation[7,8]. Liu et al. took into account the phase changes of CO<sub>2</sub> in the wellbore, using the Peng-Robinson equation of state to establish a more accurate coupled calculation model for wellbore temperature and pressure[9]; Dou et al. conducted research on the distribution of temperature and pressure in the wellbore during CO<sub>2</sub> injection, using the Span-Wagner equation of state based on Helmholtz free energy to establish a coupled calculation model, and also analyzed the impact of injection temperature, pressure, velocity, and time on the bottom-hole temperature and pressure, emphasizing the sensitivity analysis of injection parameters[10]. Zhang et al. further studied the distribution of temperature and pressure in the wellbore during CO<sub>2</sub> injection, and the model not only predicted the wellbore temperature and pressure but also could be used for temperature and pressure prediction during the drilling and fracturing process with supercritical CO<sub>2</sub>, emphasizing the significant impact of injection temperature and pressure on the bottom-hole temperature and pressure[11]. These studies have promoted the accuracy of the wellbore temperature and pressure model for CO<sub>2</sub> injection wells and the development of optimized injection parameters.

At present, the main method for optimizing CCUS injection parameters is numerical simulation. Numerical simulation methods optimize the injection parameters by establishing models for the wellbore, considering the phase changes of CO<sub>2</sub> in the wellbore and the impact of different injection parameters on the temperature and pressure profiles[12,13]. Ding et al. proposed an automatic optimization method for the CO<sub>2</sub> flooding and storage process based on low-permeability reservoirs, taking a typical well group in a low-permeability reservoir in Northern Shaanxi as a case study to explore the sensitivity of different injection methods and target functions, but it focused more on the optimization of injection parameters in the reservoir and did not optimize the injection and production parameters in the wellbore[4]. Shi et al. proposed an optimization method for CO<sub>2</sub> injection parameters, using orthogonal search to find the optimal wellhead fluid temperature and well structure parameters, but this method was inefficient and difficult to obtain the optimal parameter combination. In view of the limitations of traditional optimization methods in dealing with multi-objective optimization problems, they cannot achieve efficient and accurate global optimization[14]. This paper introduces an intelligent optimization method for CCUS injection strategy, by establishing a coupled temperature and

pressure model of the injection process, achieving flow simulation of the wellbore injection process; based on the NSGA-II algorithm for intelligent optimization of well injection parameters and well structure. By automatically optimizing the combination of well structure parameters and fluid injection parameters according to the given bottom-hole temperature and bottom-hole pressure, it not only provides a new idea for the optimization of injection parameters in CCUS technology but also lays a solid foundation for achieving more efficient and economical carbon storage and resource management strategies.

## 2. REQUIREMENTS OF PAPER STRUCTURE

Considering the complexity of CO<sub>2</sub> fluid flow in the wellbore, the assumptions for designing the CO<sub>2</sub> injection well model in this paper are as follows:

(1) there is no eccentricity in the wellbore, and the tubing is well-sealed;

(2) CO<sub>2</sub> flows one-dimensionally in the wellbore, with only radial heat transfer considered, and the temperature and pressure at all points on the same cross-section are equal, with the fluid properties remaining constant;

(3) heat transfer within the wellbore is one-dimensional and steady-state, while the heat transfer from the outer edge of the cement sheath to the formation is one-dimensional and unsteady;

(4) the influence of casing couplings on heat transfer is not considered;

(5) the physical parameters of the formation are constant with temperature and depth.

### 2.1 Model of the injector temperature and pressure

#### 2.1.1 Wellbore Temperature Model

During the CO<sub>2</sub> injection process, taking the wellhead as the coordinate origin, and considering an incremental microelement  $dz$  at any depth  $Z$  in the wellbore, the heat absorbed by the microelement can be expressed as:

$$dQ = MC_p dT \quad (1)$$

Under steady-state heat transfer conditions, the heat exchange in the radial direction between the wellbore infinitesimal element at any depth  $Z$  and the surrounding environment is:

$$dQ_1 = 2\pi r_{to} U_{to} (T_f - T_h) dz \quad (2)$$

For an infinitesimal element of the wellbore at any given depth, the radial differential equation for unsteady-state heat conduction within the surrounding environment is:

$$\frac{\partial^2 T_e}{\partial r^2} + \frac{1}{r} \frac{\partial T_e}{\partial r} = \frac{1}{\alpha} \frac{\partial T_e}{\partial \tau} \quad (3)$$

Using the semi-analytical method proposed by Ramey[15] for the solution, and introducing the dimensionless heat transfer function  $f(t_D)$ , the radial heat flux at the interface between the cement annulus and the formation within the wellbore infinitesimal element is given by:

$$dQ_2 = \frac{2\pi\lambda_e(T_h - T_e)dz}{f(t_D)} \quad (4)$$

According to the principle of energy conservation, the heat absorbed by the wellbore infinitesimal element at any depth is equal to the radial heat exchange quantity and also equal to the radial heat flux at the interface between the cement annulus and the formation:

$$dQ = dQ_1 = dQ_2 \quad (5)$$

Transforming the aforementioned equation yields the temperature gradient equation for the fluid within the wellbore:

$$\frac{dT_f}{dz} = \frac{2\pi r_{to} U_{to} \lambda_e}{[\lambda_e + r_{to} U_{to} f(t_D)] M C_p} (T_f - T_e) \quad (6)$$

#### 2.1.2 Wellbore Pressure Field Model

Similarly, selecting an infinitesimal element of the wellbore at any depth, one can derive from the continuity equation of the fluid:

$$\rho dv + v d\rho = 0 \quad (7)$$

Additionally, the flow of CO<sub>2</sub> within the tubing satisfies the momentum balance equation:

$$dp = \rho g dz \cos \theta + \frac{f \rho v^2}{4r_{ti}} dz - \rho v dv \quad (8)$$

In the formula:  $\rho$  is the density of CO<sub>2</sub>, which is dependent on temperature and pressure, measured in kg/m<sup>3</sup>;  $v$  is the flow velocity of the CO<sub>2</sub> fluid within the infinitesimal segment, measured in m/s.

By combining the aforementioned equations, one can obtain the pressure gradient equation within the wellbore:

$$\frac{dp}{dz} = \rho g \cos \theta + \frac{f \rho v^2}{2d_{ti}} + \rho v \frac{dv}{dz} \quad (9)$$

## 2.2 Friction Factor

Table1. Friction Factor calculation model in different Reynolds numbers

Reynolds numbers	Calculation Formulas
<2300	$f = \frac{64}{Re}$
2300~3400	$f = 0.06539 \times \exp \left[ - \left( \frac{Re - 3516}{1248} \right)^2 \right]$
3400~ $2 \times 10^6$	$\frac{1}{\sqrt{f}} = -2.34 \times \lg \left\{ \frac{\varepsilon}{1.72d_{ti}} - \frac{9.26}{Re} \times \lg \left[ \left( \frac{\varepsilon}{29.36} \right)^{0.95} \right] + \left( \frac{18.35}{Re} \right)^{1.108} \right\}$

### 2.2.1 Dimensionless Heat Transfer Coefficient

The function  $f(t_D)$  is a dimensionless heat transfer function that varies with time, and the Hasan[21] formula, which has a higher accuracy, is selected.

$$f(t_D) = \begin{cases} 1.1281\sqrt{t_D}(1 - 0.3\sqrt{t_D})(t_D \leq 1.5) \\ (0.4063 + 0.5\ln t_D) \times (1 + 0.6/t_D)(t_D > 1.5) \end{cases} \quad (10)$$

The dimensionless time  $t_D$  is calculated as follows.

$$t_D = t\alpha_e/r_w^2 \quad (11)$$

### 2.2.2 Friction Factor

The friction factor  $f$  characterizes the magnitude of frictional losses between the CO<sub>2</sub> fluid flow in the casing and the wall during the calculation process. It is calculated according to the formula proposed by Wang[22], which is applicable to all ranges of Reynolds numbers, as shown in Table 1.

### 2.2.3 CO<sub>2</sub> Physical Properties

In current research for calculating the physical properties of CO<sub>2</sub>, methods such as the Pen-Robinson equation[16], the Soave-Redlich-Kwong equation of state[17], the Span-Wagner model[18], the Vesovic

model[19], and the Fenghour equation[20] are commonly used. After an optimization process comparing different calculation methods for physical properties, the author has established a CO<sub>2</sub> property calculation model for the injection well, as shown in Table 1.

### 2.3 Objective Functions and Constraints

#### 2.3.1 Optimization Objectives

The optimization objectives for CO<sub>2</sub> injection parameters focus on two aspects: the difference between the actual and target bottom-hole temperatures, and the difference between the actual and target bottom-hole pressures. Based on the CO<sub>2</sub> injection well model designed in this paper, it enables the calculation of temperature, pressure, and phase state along the wellbore. Subsequently, by comparing the differences between the bottom-hole temperature and pressure with the target values, the optimization objectives of this paper are as follows:

$$\begin{cases} \min f_1 = |P_{wf} - P'_{wf}| \\ \min f_2 = |T_{wf} - T'_{wf}| \end{cases} \quad (12)$$

Table 2. CO<sub>2</sub> property calculation model for injection well

No.	Parameters	Calculation Formulas
1	CO <sub>2</sub> Density[18]	$\frac{M \cdot p(\delta, \tau)}{\rho RT} = 1 + \delta\phi'_\delta$
2	CO <sub>2</sub> Viscosity[20]	$\eta_0(T) = \frac{1.00697T^{1/2}}{G_\eta^*(T^*)}$
3	Specific Heat Capacity[18]	$C_p(\delta, \tau) = R[-\tau^2(\Phi_{\tau\tau}^o + \Phi_{\tau\tau}^r) + \frac{(1 + \delta\Phi_\delta^r - \delta\tau\Phi_{\delta\tau}^r)^2}{1 + 2\delta\Phi_\delta^r + \delta^2\Phi_{\delta\delta}^r}]$
4	Joule-Thomson Coefficient[18]	$J(\delta, \tau) = \frac{1}{R\rho} \left[ \frac{-(\delta\Phi_\delta^r + \delta^2\Phi_{\delta\delta}^r + \delta\tau\Phi_{\delta\tau}^r)}{(1 + \delta\Phi_\delta^r - \delta\tau\Phi_{\delta\tau}^r)^2 - \tau^2(\Phi_{\tau\tau}^o + \Phi_{\tau\tau}^r)} \right] * (1 + 2\delta\Phi_\delta^r + \delta^2\Phi_{\delta\delta}^r)$
5	Thermal Conductivity[19]	$\lambda(\rho, T) = \lambda_0(T) + \Delta\lambda(\rho) + \Delta\lambda_c(\rho, T)$

### 2.3.2 Constraints

In this paper, the parameters to be optimized include constraints on injection parameters and well structure parameters. In terms of injection parameters, the main aspects include the injection pressure  $P_{in}$ , injection temperature  $T_{in}$ , and injection rate  $Q_{in}$  of  $CO_2$ , among other injection parameters, which need to meet the actual conditions of the oilfield site.

$$\begin{cases} P_{min} < P_{in} < P_{max} \\ T_{min} < T_{in} < T_{max} \\ Q_{min} < Q_{in} < Q_{max} \end{cases} \quad (13)$$

In terms of well structure materials, the main aspects include the type of tubing used, whether to use conventional oil pipes or insulated oil pipes. The constraints are as follows:

$$T_{type} = \begin{cases} 0, & \text{conventional oil pipeline} \\ 1, & \text{insulated oil pipeline} \end{cases} \quad (14)$$

## 3. AN EDA-NSGA-II BASED OPTIMIZATION MODEL FOR $CO_2$ INJECTION PARAMETERS

### 3.1 The NSGA-II Algorithm

To derive the optimal  $CO_2$  injection parameters that achieve the best bottom-hole temperature and pressure effects, the NSGA-II algorithm is employed to optimize the injection parameters. The NSGA-II algorithm is widely used for solving multi-objective optimization problems [24]. Based on the original NSGA algorithm, it introduces fast non-dominated sorting to rank individuals in the population according to their fitness function values. It also uses a crowding distance algorithm to ensure that individuals in the population are evenly distributed in the solution space, preventing local convergence. Additionally, it employs an elitism strategy to retain the best individuals in each generation to improve the quality of the solution and the stability of the algorithm. The main features of the algorithm are as follows.

#### 3.1.1 Fast Non-Dominated Sorting

In the NSGA-II algorithm, all individuals are sequentially classified into different levels of fronts based on the dominance relationship. The front rank of an individual reflects the quality of the individual. If the two compared individuals have different front ranks, the lower the rank number, the more preferred the individual is in the selection process.

#### 3.1.2 Crowding Distance Algorithm

Calculation of crowding distance. Individuals of the same rank need to be further measured by the crowding distance indicator. After the dominance rank of each individual is determined, the crowding distance must be

calculated. Among individuals of the same front rank, the larger the crowding distance, the more preferred the individual is in the non-dominated sorting sequence. The formula for calculating crowding distance is as follows:

$$\begin{cases} D(i, j) = \frac{f_j(i+1) - f_j(i-1)}{f_j^{max} - f_j^{min}} \\ D(i) = \sum_{j=1}^n D(i, j) \end{cases} \quad (15)$$

In the formula,  $D(i, j)$  represents the distance of individual  $i$  in objective  $j$ ;  $f_j^{max}$  and  $f_j^{min}$  are the maximum and minimum values for objective  $j$ , respectively;  $f_j(i+1)$  and  $f_j(i-1)$  are the neighboring values adjacent to individual  $i$  in objective  $j$ ;  $D(i)$  is the crowding distance of individual  $i$ , which is the sum of the distances of individual  $i$  across all objectives. The crowding distance of the boundary points in each front is set to infinity.

#### 3.1.3 Elite Preservation Strategy

In the NSGA-II algorithm, an elitism preservation strategy is employed to select outstanding individuals for the new generation. This strategy involves merging the parent and offspring populations to form a new population whose size is twice that of the original population. Then, the combined population undergoes calculations for front ranking and crowding distance, obtaining a ranking of all individuals' quality. According to the comparison rules that determine excellence, outstanding individuals are sequentially filled into the next generation's population until the size of the next generation's population returns to the size of the merged population before the split.

### 3.2 The EDA-NSGA-II Algorithm

Estimation of Distribution Algorithm (EDA) is a class of evolutionary algorithms that generate new solutions by statistically learning and modeling the distribution of the current population, rather than relying on traditional crossover and mutation operations. EDA begins by estimating the distribution of superior individuals, constructs a probability model, and then generates new individuals based on this model. This approach helps to maintain good genes while enhancing the algorithm's global search capability and convergence speed. NSGA-II uses traditional mutation operators to generate offspring populations.

The allocation of parameters, such as replacement rate, crossover rate, and mutation rate, determines the final performance of the algorithm. For inexperienced users, setting the appropriate parameters is not easy.

Moreover, neglecting the relationships between variables within individuals can lead to aimlessness in searching for optimal individuals. Therefore, we employ the EDA algorithm to improve the NSGA-II algorithm.

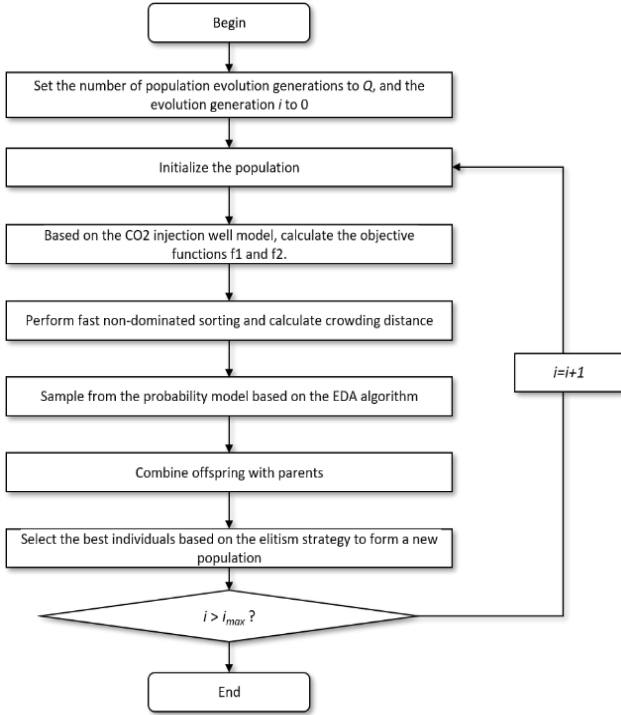


Fig. 1. EDA-NSGA-II algorithm flowchart

The procedural steps delineated from step 1 through step 5 represent the conventional operational mechanisms inherent to the NSGA-II framework. Post the culmination of step 5, an ensemble of elite individuals, denoted as  $D_u$ , is meticulously curated. This selection is predicated on their exceptional fitness metrics coupled with their contribution to the diversity of the population, thereby forming an apt learning dataset for the subsequent EDA phase. The EDA then engenders a probabilistic model that encapsulates the collective behavior of these distinguished individuals.

A joint probability distribution  $P_u(X)$  for  $X = (x_1, \dots, x_{|\zeta|})$  is induced. Here we use the algorithm UMDA (univariate marginal distribution algorithm) to construct probabilistic model. The joint probability distribution  $P_u(X)$  is induced by:

$$p_u(X) = p_u(X | D_u) = \prod_{i=1}^{|\zeta|} p_u(x_i) = \prod_{i=1}^{|\zeta|} \frac{\sum_{j=1}^M \delta_j(x_i = a_i | D_u)}{M} \quad (16)$$

In the formula,  $a_i$  is the value of the  $i$ th bit, which equals one or zero.  $M$  is the number of individuals included in the  $D_u$ . After the joint probability distribution  $P_u(X)$  is available, offspring  $O_u$  with  $Q$  individuals is generated by randomly sampling with the

joint probability  $P_u(X)$ . Finally according to crowded tournament selection, select best  $Q$  individuals as next population from the combination of  $PO_u$  and  $O_u$ .

## 4. EXPERIMENTS AND ANALYSIS

### 4.1 Case Study of CO<sub>2</sub> Injection Well

In order to validate the effectiveness of the injection well model and the optimization model, the temperature and pressure measurement data from an injection well in a certain oilfield in Jiangsu are used as the verification data for the injection well model, followed by the optimization work of CO<sub>2</sub> injection parameters.

Table 3. Basic parameters of the injection well

Parameter	Value
Well Depth, m	3100
Tubing Inner Diameter, mm	62
Tubing Outer Diameter, mm	73
Casing Inner Diameter, mm	124.37
Casing Outer Diameter, mm	137
Injection Pressure, MPa	30
Injection Temperature, K	293.15
Surface Temperature, K	288.15
Geothermal Gradient, K/m	0.03
Gas Injection Rate, t/d	55.4

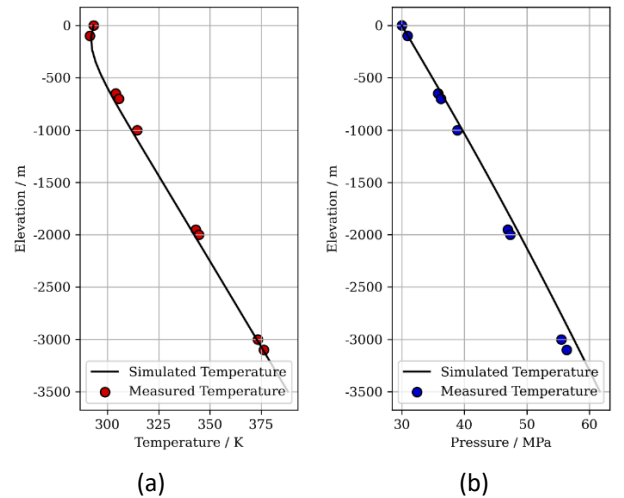


Fig. 2. CO<sub>2</sub> injection wellbore temperature and pressure profiles (a) Wellbore temperature profile (b) Wellbore pressure profile

Following the analysis of the CO<sub>2</sub> injection well temperature and pressure calculation model established in this paper, it can be observed that the model has a high degree of accuracy, with calculated results closely

matching the actual field-collected data. The relative errors are minimal. At the nine test points within the wellbore, the relative error between the actual pressure and the calculated pressure is 1.94%, and the error in the actual temperature compared to the calculated temperature is 0.46%.

#### 4.2 Analysis of Parameter Optimization Results

To validate the capability of the EDA-NSGA-II algorithm in optimizing injection well parameters, the target bottom-hole temperature is set at 373K, and the bottom-hole pressure is set at 50MPa. The algorithm's population size  $Q$  is set to 50, and the maximum number of iterations  $i_{max}$  is set to 200. In the NSGA-II algorithm, the crossover probability  $R_c$  is set to 0.8, and the mutation probability  $R_m$  is set to 0.1. When designing the parameters for the EDA-NSGA-II algorithm, it is the same as the NSGA-II algorithm, with 80% of individuals generated by the EDA method, and the mutation probability is  $R_m$  0.1. The search range for optimization is as follows:

Table 4. Main injection parameters

Injection Parameter	Injection Temperature	Injection Pressure	Injection Flow Rate
Upper Limit	233.15K	10MPa	20 t/d
Lower Limit	298.15K	40MPa	50 t/d

Comparative experiments were conducted for both the NSGA-II and EDA-NSGA-II algorithms. Figure 3 illustrates the Pareto optimal solution sets obtained after optimizing the CO<sub>2</sub> injection well case under identical parameter settings with the two algorithms. It can be observed from the figure that, in comparison with the NSGA-II algorithm, the EDA-NSGA-II algorithm yields solutions of higher quality, with better convergence and more uniform distribution. At the same level of optimization iteration, when compared with the target temperature and pressure values, the EDA-NSGA-II

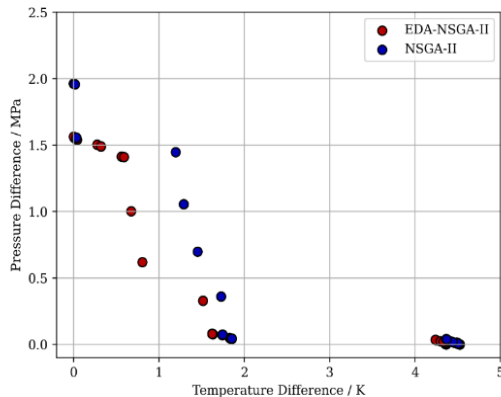


Fig. 3. Comparison of Pareto fronts of the two algorithms

algorithm achieves closer bottom-hole temperatures and pressures in the injection well.

Moving forward with a refined analysis of the EDA-NSGA-II algorithm's optimization process, we start by examining the evolution of the Pareto front at different generations of the EDA-NSGA-II algorithm, as depicted in Figure 4. Initially, individuals of the population are scattered throughout the solution space. As the number of iterations increases, the Pareto front gradually moves towards the direction of the optimal solution set. The rapid expansion of the Pareto front in the early iterations indicates that the algorithm possesses a swift convergence rate. The Pareto front in the final generations demonstrates a uniform distribution of solutions, indicating a good diversity within the population.

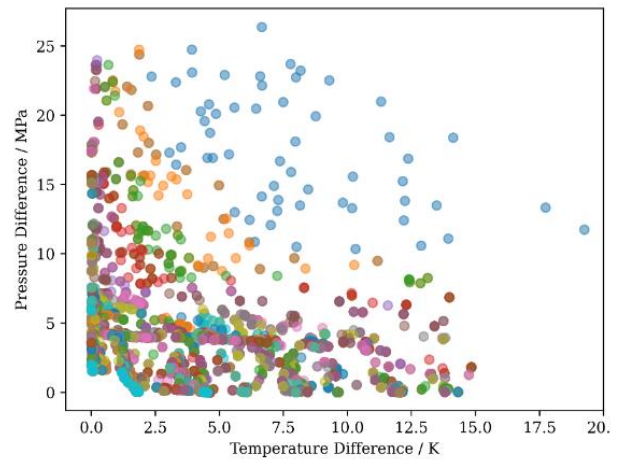


Fig. 4. Translation of EDA-NSGA-II Pareto front evolution

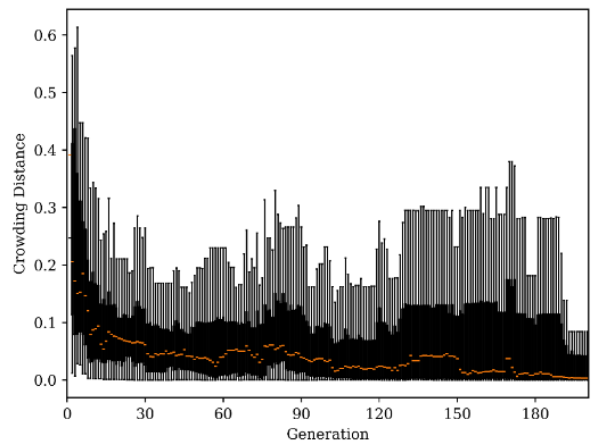


Fig. 5. Crowding distance distribution over generations

In the analysis of crowding distance, we plotted the box plots of crowding distance for each generation to assess the distribution of the population in the objective space. It can be observed from the figure that in the first 30 generations, the overall crowding distance of the population is relatively high. As the number of iterations

increases, the crowding distance gradually decreases and tends to stabilize, indicating that the population is gradually converging to the Pareto front with a more uniform distribution of solutions. At the same time, the crowding distance of the population at each generation does not decrease steadily, which is due to significant variations that occurred within those generations.

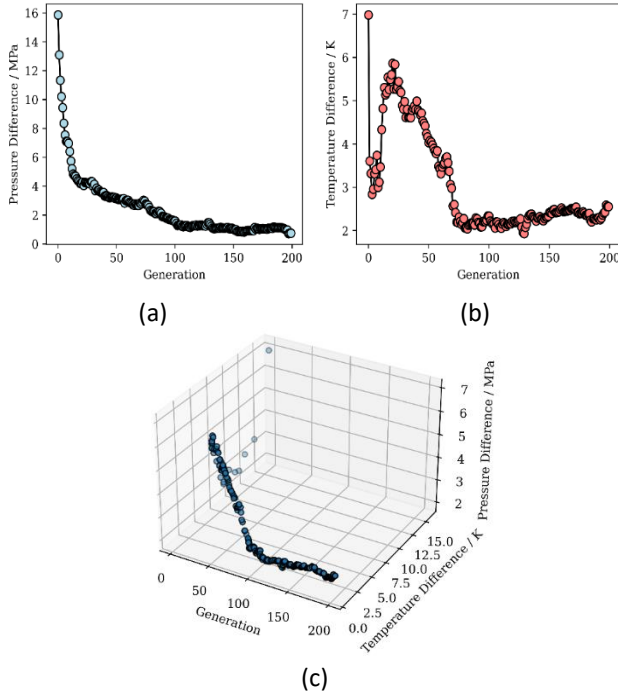


Fig. 6 The differential evolution of the temperature and pressure curve(a) Pressure difference evolution curve(b) Temperature difference evolution curve(c) Three-dimensional curves

Subsequently, the optimization effects of the EDA-NSGA-II algorithm on temperature and pressure were analyzed separately. The changes in the average temperature difference and the average pressure difference of the population are shown in the Figure 5. The curve of the average difference values of the population demonstrates the change in the overall fitness of the population during the optimization process. The gradual decrease in the average temperature and pressure differences indicates that the algorithm is continuously refining the population. However, significant fluctuations in the fitness value of the temperature difference were observed in the early generations, possibly due to greater variations in the search process of the population.

The three-dimensional curves illustrate the changes in the target values with the number of iterations. Through these curves, we can intuitively observe the trend of the two target values throughout the entire iterative process. The results indicate that as the number

of iterations increases, the target values gradually converge on the optimal solution set. In the final optimized combination of injection parameters, the difference in the downhole temperature from the target temperature is around 1K, and the difference in the downhole pressure from the target pressure is about 0.2MPa.

## 5. CONCLUSIONS

In this paper, to address the design of injection parameters for CO<sub>2</sub> Capture, Utilization, and Storage (CCUS) in Enhanced Oil Recovery (EOR) and storage operations, we propose an intelligent multi-objective optimization method based on the second-generation Non-Dominated Sorting Genetic Algorithm (NSGA-II) combined with the Estimation of Distribution Algorithm (EDA). Initially, we established a temperature and pressure calculation model for the CO<sub>2</sub> injection wellbore, which can accurately simulate the characteristics of fluid flow along the wellbore and the temperature and pressure at the bottom hole. This model is crucial for understanding the transport mechanism of CO<sub>2</sub> in the wellbore and provides a theoretical basis for the optimization of injection parameters.

Subsequently, to address the limitations of the traditional NSGA-II algorithm in the optimization of CCUS parameters, we introduced the Estimation of Distribution Algorithm (EDA) to enhance the global and purposeful search capabilities of the algorithm. The improved EDA-NSGA-II algorithm significantly improves optimization performance and convergence speed while maintaining population diversity, effectively resolving the issues of randomness and local convergence in parameter optimization.

Finally, through case analysis, we verified the effectiveness and superiority of the proposed intelligent optimization method in the design of CCUS injection parameters. Experimental results show that compared to the traditional NSGA-II algorithm, the EDA-NSGA-II algorithm can converge to the Pareto optimal solution set more quickly, and the obtained solution set is more uniformly distributed, closer to the needs of practical engineering, providing strong technical support for the implementation of CCUS projects.

## DECLARATION OF INTEREST STATEMENT

The authors declare that they have no known competing financial interests or personal relationships that could have appeared to influence the work reported

in this paper. All authors read and approved the final manuscript.

## REFERENCE

- [1] Xian Zhang; Kai Li; Qiao Ma; Jingli Fan, "Development Orientation and Prospect of CCUS Technology under the Goal of Carbon Neutrality," *China Population, Resources and Environment*, vol. 31, no. 09, pp. 29-33, 2021.
- [2] Yong Xiang; Li Hou; Meng Du; Ninghong Jia; Weifeng Lv, "Research Progress and Development Prospects of CCUS-EOR Technology in China," *Oil and Gas Geology and Recovery*, vol. 30, no. 02, pp. 1-17, 2023, doi: 10.13673/j.cnki.cn37-1359/te.202112048.
- [3] D. Y. C. Leung, G. Caramanna, and M. M. Maroto-Valer, "An Overview of Current Status of Carbon Dioxide Capture and Storage Technologies," *Renewable and Sustainable Energy Reviews*, vol. 39, pp. 426-443, November 2014, doi: 10.1016/j.rser.2014.07.093.
- [4] Shuaiwei Ding; Yi Xi; Jian Liu; Meng Zhang; Linlin Ji; Hongyan Yu; Yanfang Gao, "Automatic Optimization of CO<sub>2</sub> Flooding and Storage in Low Permeability Reservoirs Based on Particle Swarm Algorithm," *Journal of China University of Petroleum (Edition of Natural Science)*, vol. 46, no. 04, pp. 109-115, 2022.
- [5] Geng Gong; Yi Li; Dong Tang; Hao Yu; Zhongming Jiang, "Optimization Study on CO<sub>2</sub> Geological Sequestration Injection Scheme under THM Coupled Conditions," *Chinese Journal of Geotechnical Engineering*, vol. 31, no. 03, pp. 1084-1096, 2023, doi: 10.13544/j.cnki.jeg.2021-0034.
- [6] Baobing Shang; Xinwei Liao; Ning Lu; Huan Wang; Xiangji Dou; Yifan He; Baozhe Chen, "Optimization of CO<sub>2</sub> Water-Alternating-Gas Injection and Production Parameters: A Case Study of the Chang 6 Oil Reservoir in the Wangyao Area of the Ansai Oilfield," *Oil and Gas Geology and Recovery*, vol. 21, no. 03, pp. 70-72+77+115-116, 2014, doi: 10.13673/j.cnki.cn37-1359/te.2014.03.019.
- [7] A. T. Singhe, J. R. Ursin, J. Henniges, G. Pusch, and L. Ganzer, "Modeling of Temperature Effects in CO<sub>2</sub> Injection Wells," *Energy Procedia*, vol. 37, pp. 3927-3935, January 2013, doi: 10.1016/j.egypro.2013.06.291.
- [8] E. Lindeberg, "Modelling Pressure and Temperature Profile in a CO<sub>2</sub> Injection Well," *Energy Procedia*, vol. 4, pp. 3935-3941, January 2011, doi: 10.1016/j.egypro.2011.02.332.
- [9] Xiaodong Wu; Qing Wang; Yanfeng He, "Coupled Calculation Model of Wellbore Temperature and Pressure Field Considering Phase Change in CO<sub>2</sub> Injection Wells," *Journal of China University of Petroleum (Edition of Natural Science)*, vol. 33, no. 01, pp. 73-77, 2009.
- [10] Liangbin Dou; Gensheng Li; Zhonghou Shen; Chunfang Wu; Gang Bi, "Research on Prediction Model and Influencing Factors of Wellbore Temperature and Pressure in CO<sub>2</sub> Injection Wells," *Oil Drilling Techniques*, vol. 41, no. 01, pp. 76-81, 2013.
- [11] Yonggang Zhang; Yi Luo; Yuelong Liu; Yulin Lu; Kaipeng Wei, "Study and Field Application of Temperature and Pressure Distribution Model in CO<sub>2</sub> Injection Wells," *Petroleum Geology and Oil Recovery*, vol. 26, no. 02, pp. 108-113, 2014.
- [12] K. Musayev, H. Shin, and V. Nguyen-Le, "Optimization of CO<sub>2</sub> Injection and Brine Production Well Placement Using a Genetic Algorithm and Artificial Neural Network-Based Proxy Model," *International Journal of Greenhouse Gas Control*, vol. 127, p. 103915, July 2023, doi: 10.1016/j.ijggc.2023.103915.
- [13] T. Goda and K. Sato, "Global Optimization of Injection Well Placement Toward Higher Safety of CO<sub>2</sub> Geological Storage," *Energy Procedia*, vol. 37, pp. 4583-4590, January 2013, doi: 10.1016/j.egypro.2013.06.366.
- [14] Zaihong Shi; Changzhi Lin; Bu'e Wang; Jianzheng Su; Yaru Wang; Aiping Shi; Qiufen Chen, "A Method for Determining the Flow State in the Wellbore of a CO<sub>2</sub> Injection Well and Optimizing the Parameters," November 14, 2012.
- [15] H. J. Ramey Jr., "Wellbore Heat Transmission," *Journal of Petroleum Technology*, vol. 14, no. 4, pp. 427-435, 1962.
- [16] L. H. Pan, C. M. Oldenburg, Y. S. Wu, et al., "Wellbore Flow Model for Carbon Dioxide and Brine," *Energy Procedia*, vol. 1, no. 1, pp. 71-78, 2009.
- [17] G. Soave, "Rigorous and Simplified Procedures for Determining the Pure-Component Parameters in the Redlich-Kwong-Soave Equation of State," *Chemical Engineering Science*, vol. 35, no. 8, pp. 1725-1730, 1980.
- [18] R. Span and W. Wagner, "A New Equation of State for Carbon Dioxide Covering the Fluid Region from the Triple-Point Temperature to 1100 K at Pressures up to 800 MPa," *Journal of Physical and Chemical Reference Data*, vol. 25, no. 6, pp. 1509-1596, 1996.
- [19] V. Vesovic, W. A. Wakeham, G. A. Olchowy, et al., "The Transport Properties of Carbon Dioxide," *Journal of Physical and Chemical Reference Data*, vol. 19, no. 3, pp. 763-808, 1990.
- [20] A. Fenghour, W. A. Wakeham, V. Vesovic, "The Viscosity of Carbon Dioxide," *Journal of Physical and Chemical Reference Data*, vol. 27, no. 1, pp. 31-44, 1998.
- [21] A. R. Hasan and C. S. Kabir, "Aspects of Wellbore Heat Transfer during Two-Phase Flow," *SPE Production & Facilities*, vol. 9, no. 3, pp. 211-216, 1994.

[22] Z. Y. Wang, B. J. Sun, J. T. Wang, et al., "Experimental Study on the Friction Coefficient of Supercritical Carbon Dioxide in Pipes," *International Journal of Greenhouse Gas Control*, vol. 25, pp. 151-161, 2014.

[23] L. Min, M. Liu, D. Xi, et al., "Study of Supercritical CO<sub>2</sub> Physical Property Calculation Models," *Frontiers in Energy Research*, vol. 10, 835311, 2022.

[24] Alawode K O, Adegboyega G A, Abimbola Muhideen J. NSGA-II/EDA hybrid evolutionary algorithm for solving multi-objective economic/emission dispatch problem[J]. *Electric power components and systems*, 2018, 46(10): 1160-1172.